Published in final edited form as:
Brain Stimul. 2014 ; 7(3): 476–482. doi:10.1016/j.brs.2014.01.006.

Histological Assessment of Thermal Damage in the Brain following Infrared Neural Stimulation

Mykyta Mikhailovich Chernov[1], **Gang Chen**, and **Anna Wang Roe**
Department of Psychology, Vanderbilt University, 111 21st Ave South, 301 Wilson Hall, Nashville TN 37240

Keywords

Infrared Neural Stimulation; Thermal Damage; Non-human primate

Introduction

Within the past two decades, much progress has been made in the area of brain machine interfaces, with the goal of restoring function to impaired neural networks or otherwise altering or enhancing brain function. Central to these approaches has been the activation (or inactivation) of brain tissue via electrical stimulation. However, this conventional method suffers from lack of spatial precision due to current spread. Implantation of newer microelectrode arrays offers better current control but allows for only sparse coverage of the neuronal circuit due to the trauma caused by implantation of a dense wire array. (1) A fundamentally different approach is the use of light to stimulate neurons, a technique that overcomes the problem of current spread and offers focal and spatially specific neural stimulation. Recent advances capable of rendering neurons sensitive to light (by introducing algal photosensitive ion channels from the opsin protein family into the mammalian genome using recombination techniques or viral vectors), a method known as optogenetics, has revolutionized the field of neuroscience research. (2) Optogenetics allows one to focally stimulate specific neuronal populations (e.g. excitatory or inhibitory neurons). However, the prospect of using optogenetics as a clinical tool is still uncertain, due to concerns over the safety of gene therapy in human patients.

Another approach to using light to stimulate neural tissue is infrared neural stimulation (INS). This method employs brief pulses of infrared (1000–3000 nm) light to stimulate

[1]Corresponding author. Phone: (603)-306-6263 Mykyta.M.Chernov@Vanderbilt.edu.

Financial Disclosure
The authors have no financial disclosures to report.

Some of this work has been presented in abstract form :
Chernov M, Chen G, Roe AW (2013) Histological assessment of thermal damage thresholds for infrared neural stimulation of the brain. SPIE Photonics West, San Francisco, CA.

neurons. (3) Neuronal excitability by INS has been demonstrated in a variety of neuronal tissues, ranging from embryonic hearts to the human PNS and does not require chemical or genetic manipulations. (8–11) The transduction of optical pulses leads to changes in the transmembrane potential and is driven by the thermal gradient induced by the absorption of infrared light. (4) Recent *in vitro* studies using artificial lipid membranes and *Xenopus* oocytes have shown that the mechanism behind INS in these preparations is due to the temperature-dependent redistribution of capacitative charges across the lipid membrane itself. (5) The effect can be large enough to drive the membrane past the depolarization threshold. *In vivo*, in addition to the effects on the membrane itself, INS may also alter the conductance of various ion channels, many of which (the TRPV channel family, for example) are exquisitely temperature-sensitive. (6) The presence of these channels is one explanation for the observed differences to INS in terms of radiant exposure across various types of excitable membranes. (7) The spatial specificity of INS comes from: 1) the fact that its action is confined to the area being illuminated and 2) that lateral spread is minimal, due to low scattering, high absorption of mid-infrared light and the short duration of the light pulse (10^{-4} to 10^{-3} s) compared to the thermal relaxation time of about 90 ms. (4) Around the 1900 nm absorption peak for water, (other peaks exist around 1470 and 3000 nm) the absorption coefficient is 100 cm^{-1} and very focal activation can be achieved by delivering light to the region of interest via an optical fiber (e.g. 100–200 microns in diameter). (12)

Although INS has several advantages over electrical and optogenetic stimulation methods, its safety in the CNS needs to be fully assessed before it can be used in the clinic. The primary concern is thermally induced damage. Two questions need to be answered. First, what is the maximum temperature rise, T_{max}, tolerated by neural tissue? And, second, what is the parameter space for INS which produces temperatures below T_{max}? Neither of the two questions is easy to answer. The lower limit for T_{max} must lie somewhere around 41–42° C, a point at which thermal damage to tissue has been observed in patients with high fevers and in animal studies. (13) Since INS is pulsed, and not continuous, this figure is probably too low. For example, human skin can be exposed for several minutes to immersion in water at temperatures of 48° C, and can even tolerate temperature of up to 60° C if the exposure is shortened to several seconds. (14) The upper limit is around 100° C, the boiling point of water, at which immediate damage is observed. This range of 60° C is too broad to be useful.

The temperature rise produced during INS is also not well established. It is difficult to measure empirically. Reported values differ considerably and have been obtained in different tissues, and, therefore, may not be comparable. (4, 15) Moreover, the temperature during INS is dependent on a number of factors, including the repetition rate of the stimulation pulses and the energy delivered per pulse. A further complication arises from the fact that, at high pulse rates, the heat generated by each pulse does not dissipate completely and therefore the steady state temperature of the tissue increases. Given the rather large parameter space, the question is most easily addressed by numerical models, a number of which have been published. (16–19) However, these models often do not include a refined description of the tissue being stimulated, treating it as a homogeneous aqueous environment.

Rather than trying to estimate T_{max} tolerated by the tissue and predict whether the particular INS paradigm used exceeds it, we took an empirical approach and looked for signs of tissue damage following INS, varying just one parameter, the radiant exposure per pulse. A previous study has examined the safety of applying INS to peripheral nerves in rats (20). Our study differs significantly in that it employs both the INS sequence and its mode of delivery in a way that is directly applicable to neuroscience experiments in non-human primates, a primary model for human applications. (21) In this study, we obtain an approximate threshold above which thermal damage is observed in histological preparations for this particular INS sequence, characterize the changes in the severity of damage as a function of radiant exposure, and propose an underlying mechanism responsible for this damage.

Methods

Stimulation Sequence

The INS stimulation paradigm that we tested was developed in view of its potential application, namely, modulation of cortical activity in awake, behaving non-human primates. It is structured as a series of short INS bursts with a longer interstimulus interval between, corresponding to a number of trials back-to-back within one experimental session (Fig 1). The bursts are 0.5 s in duration and consist of a continuous train of 0.25 ms wide pulses delivered at a frequency of 200 Hz. These pulse trains are sufficient for eliciting neuronal activation observed using calcium reporter dyes and electrophysiological and optical imaging of hemodynamic response measurements in rodents. (10) The only variable in the stimulation sequence was the radiant exposure per pulse. Since the pulse duration remained constant, this was achieved by altering the laser diode current and thus peak powers were adjusted to deposit from 0.3 to 0.9 J/cm^2 for each pulse. The inter-stimulus interval between the 0.5 s pulse trains was 5 seconds, and was chosen because it was deemed long enough to allow for the residual heat to dissipate, yet short enough to allow for a large number of stimulations to be performed within a reasonable amount of time. The stimulation sequence was run for thirty minutes, resulting in approximately 36000 individual pulses being delivered to the brain. Since the damage threshold for the stimulation sequence was not known in advance, we used high-energy single pulses (2 or 5 J/cm^2 delivered in 2 or 5 ms, respectively) to estimate the upper limit for the energies required. Single pulses of either magnitude produced large lesions; therefore we decreased the diode current by a factor of two or more for the pulse sequence.

Experimental Setup

We carried out INS stimulation in five Long-Evans Rats (*Rattus norvegicus*) and two squirrel monkeys (*Saimiri sciureus*). All procedures were approved by the Vanderbilt University Institutional Animal Care and Use Committee. The animals were anesthetized with standard procedures (urethane for rats or isoflurane in oxygen/nitrous oxide mixture for the squirrel monkeys) and placed in a stereotaxic frame. A craniotomy and durotomy was performed and the brain covered with an approximately 0.2 mm thick sheet of optically transparent silicone, secured at the edges with a 4% solution of agar in saline. INS was carried out using a solid state 1875 nm laser as the light source (Capella, Lockheed-Martin

Aculight), delivered to the cortex via a 200 micron diameter multimode optical fiber with a numerical aperture of 0.22 (Ocean Optics P200-2-VIS-NIR) positioned approximately normal to the brain surface using a micromanipulator. The laser output was calibrated before each experiment using a Power Max 500D power meter with a PM3 detector (Coherent). Cerebral cortex in each animal was stimulated at 5–6 different locations. At the conclusion of the experiment, the animals were euthanized, perfused with 4% formalin and their brains were removed for histological processing.

Histological Sample Preparation and Analysis

The rat brain samples were paraffin mounted, sliced at thickness of 6 microns and stained with hematoxylin and eosin. In case of the squirrel monkey brains, 50 micron- thick frozen sections were prepared and stained with cresyl violet. The samples were photographed using a digital camera mounted on a microscope with a motorized translation stage, capable of generating a high-resolution photomontage from multiple images. In case of the rat brains, most lesions were readily visualized and their positions relative to each other were confirmed based on the *in vivo* photographs. In the squirrel monkeys, all of the lesions were visible and electrolytic microlesions created *in vivo* were used to aid in image registration. The lesions were approximately parabolic in shape, and a consistent pattern of 3 different zones of damage was observed. The extent of the lesions was quantified by measuring the width of the zones at the surface (the widest point) as well as the maximal depth below the cortical surface.

Results

Rats

When the energy per pulse reached a threshold of approximately 0.4 J/cm^2, INS caused clearly identifiable lesions in the rat brain in histological specimens. Lesions produced using radiant exposures of 0.6 J/cm^2 or higher were usually visible *in vivo* as well. Figure 2 shows a representative cortical area that received INS *in vivo*. Of the three locations that received INS, visible signs of damage occurred at sites A and B. Damage appeared as blanching of the tissue (often ring-like rather than circular), minor bleeding and thermal cauterization of superficial blood vessels; this may have caused localized ischemia in addition to thermal damage. At the powers used, the visible damage was focal, not exceeding the approximately 200 micron diameter of the optical fiber core used to deliver the light.

Figure 3A shows a schematic representation of the lesions observed following suprathreshold radiant exposures. The lesions exhibited 3 visually identifiable zones of damage extending outward from the center and down below the cortical surface, labeled as zones 1, 2 and 3. Unaffected tissue is labeled as zone 4. These three components can be clearly seen in a typical lesion at low and high magnifications (Figs 3B and 3C). In zone 1, the damage was primarily characterized by neuronal necrosis, with intensely basophilic pyknotic nuclei, surrounded by an eosinophilic perikaryon (Fig 3C). In zone 2, there is extensive vacuolization due to shrinking of both the neuronal bodies and the surrounding tissue (Fig 3C). The nuclei are basophilic and pyknotic and the neurons themselves appear similar to the ones observed after acute hypoxic ischemic injury. (22) In zone 3, the majority

of neurons are normal, with the exception of a few so-called “dark neurons” (Fig 3D). These are characterized by a dark basophilic cell body as well as a corkscrew-shaped dendrite. Such neurons are often regarded as artifacts observed in specimens which were inadequately perfused or suffered from post-mortem compression during brain removal. (23) However, in our samples, these neurons were found exclusively around the laser-induced lesions, suggesting that the two are somehow linked. Such dark neurons are also a hallmark of certain conditions such as hypoglycemia and status epilepticus; their abnormal appearance seems to be reversible in some cases, which is taken as an indication of cell injury rather than outright cell death. (22)

The three zones of damage described above were consistently observed in INS-induced lesions produced with exposure to laser radiation from 0.4 to 0.8 J/cm^2. No signs of damage were observed at the radiant exposure of 0.3 J/cm^2. There were no qualitative differences between the lesions due to radiation of different magnitudes, suggesting similar mechanisms of tissue damage at these radiant exposures. We found that the size of the lesions was positively correlated to the radiant exposures used (Fig 4A). With greater radiant exposures, the lesions became progressively deeper but not wider, consistent with theoretical models of energy deposition into tissue via an optical fiber. (17) We found that this held true for all three zones of damage observed (the results are quantified in Figure 4B). The downward expansion of each of zones 1, 2 and 3 occurred at approximately the same rate, but the overall rate of expansion decreased at the upper range of the radiant exposures tested.

The results from our initial single pulse high radiant exposure tests indicate that somewhere between the radiant exposures of 2 and 5 J/cm^2, a new damage pattern emerges. As shown in Figure 5, these high energy pulses resulted in severe shrinking of what was termed zone 1, leading to either multiple large cavities, or a single crater-like depression. Moreover, it also led to rupture of blood vessels, which caused zones 1 and 2 to become filled with blood. Single pulse lesions of 2 J/cm^2, on the other hand, are qualitatively similar to the ones obtained with our pulse sequence. These results suggest that although there may be some cumulative damage sustained by the tissue after a series of pulses, it is not responsible for the formation of the lesion pattern observed, but only modifies it.

Non-Human Primates

INS in the squirrel monkeys was performed at radiant exposures of 0.7, 0.8 and 0.9 J/cm^2. INS stimulation was applied at 12 cortical locations (3 of them shown in Figure 6). All stimulations in the squirrel monkeys produced lesions that were visible in histological preparations. Qualitatively, these lesions have a similar appearance to the ones observed in the rodent brain. The three zones of damage identified earlier are present, although, as these sections are from relatively thick frozen sections, the changes in individual cell morphology are more difficult to make out. Because of this, only the depth of zone 2 could be precisely established. Zone 2 in the cresyl violet preparation is almost transparent, appearing as a parabola-shaped gap between zone 1 and the cortical surface subjected to INS and the rest of the slice. The depth of the lesions observed correlates quite well with the data obtained from the rats. The maximal depth of zone 2 in the squirrel monkeys was 232, 382 and 437 microns for radiant exposures of 0.7, 0.8 and 0.9 J/cm^2, respectively (average of 4 data

points for each value, Fig 4B). The extent of the lesions in the monkeys was slightly smaller compared to the one observed in the rats at the same radiant exposures.

Discussion

Possible Mechanism of Damage

We found that our INS paradigm produced histologically visible lesions in the rodent brain when radiant exposures per pulse reached or exceeded 0.4 J/cm^2. All lesions have the same morphology, with the most apparent feature being a sponge-like band of tissue we call zone 2, surrounded by zones 1 and 3 where neuronal damage is found but the connective tissue itself is relatively unaffected. Zone 2 appears as a flat band (in coronal slices) on the surface of the tissue at low radiant exposures and assumes the shape of a parabola as the radiant exposure is increased. Moreover, when zone 2 is not observed, neither are zones 1 or 3. Thus, in our experience, the tissue exposed to INS either appears normal, or has a clear lesion with the morphology described above. Histologically, the sponge-like zone 2 is the most prominent feature of the lesion. Its appearance is consistent with formation of small bubbles, which could be a result of water boiling or some other mechanism of gas generation. The porous appearance of zone 2 exists in both stained and unstained histological specimens, suggesting that the lesion morphology cannot be explained by weak uptake of the stains used by the tissue. It should also be noted that the maximal increase in tissue temperature occurs in zone 1, which is closer to the fiber than zone 2. It is possible that the high temperature gradient between zones 1 and 2 is responsible for the formation of bubbles observed.

Bubble formation due to pulsed energy deposition is highly dependent on the penetration depth of the absorbing medium as well as on the duration of the pulse. We observed bubbles directly using radiant exposures of 4 J/cm^2 per pulse (single 2 ms long pulses) by immersing the optical fiber in water. No bubbles could be detected using our experimental INS pulse sequence with radiant exposures of up to 1 J/cm^2 per pulse, the maximal output achievable with our laser and optical fiber combination, although their existence cannot be ruled out without the use of high speed photographic equipment. Therefore, the mechanism responsible for the porous appearance of zone 2 remains unknown.

Even though we do not see any histological sign of thermal damage below 0.4 J/cm^2 using our INS sequence, one could argue that it is too subtle to be seen with the methods employed or that its progression is too slow to be immediately apparent after INS stimulation. However, we have other reasons to believe that INS applied with our paradigm does not cause damage severe enough to cause neurological deficits. In monkeys that have been subjected to INS over multiple sessions (many hundreds of trials) In both the anesthetized and awake states, the cortex remains healthy as assessed electrophysiologically, with optical imaging, and with fMRI. (21, 24, 25) We observe no alterations in cortical activity. Moreover, animal behavior (as assessed by visual detection and discrimination tasks involving eye movement responses) and health remain normal.

Limitations of the Study

The bulk of our experiments were carried out in rodents. In the case of the squirrel monkeys, the lesions obtained were similar in size and appearance to the ones obtained in rodents, although they were less deep at any given radiant exposure (Fig 4B). However, the depth-radiant exposure curve is steep, and even a 0.05 J/cm^2 variation in the effective radiant exposure due to factors discussed below could explain the difference between the results from the two different species. There is little reason to believe that the rodent and primate brains should have drastically different thermal damage thresholds. Of course, while the penetration depth of IR-light is similar in both animal species, the difference in the thickness of the cortical layer means that what in the monkey would be only a superficial lesion - too shallow to penetrate the neuron-containing layers of the brain - would span the depth of the entire cortex in the rat. The major source of error in our study is the presence of a layer of cerebrospinal fluid between the silicone membrane and the brain. Given that water is the main absorber of IR-light in tissue, a layer even a hundred microns thick would skew the results significantly. In our study, we positioned the optical fiber so that it exerted only light pressure against the underlying the silicone membrane in order to avoid damaging the brain, therefore some of the fluid may have remained between the silicone and the cortex. It should also be noted that we have chosen to report the magnitude of our laser stimuli as radiant exposure at the tip of the fiber, to allow for ease of comparison with other studies. Since light exits the fiber as a cone rather than a cylindrical beam, the diameter of the illumination spot, having passed through the silicone and any fluid layer present, would be larger (25% larger diameter after 0.2 mm of water, slightly less for silicone of the same thickness). However, as shown by Thompson et al. using Monte Carlo simulations of light spread in a non-absorbing medium, the majority of the radiant energy within the light cone is confined to an area centered along the fiber's optical axis and remains fairly uniform until a critical depth (about 600 microns in the case of the fiber used in this study) is reached. (18)

The goal of this study has been to identify the approximate thermal damage threshold for an INS stimulation preparation suitable for experiments on awake non-human primate subjects, as well as to characterize the lesions when suprathreshold radiant exposures are used. The thermal threshold observed here does not hold for experimental preparations that differ significantly in either the stimulation sequence, the fiber diameter, or the illumination spot size, the latter being a function of the numerical aperture, the medium separating the brain from the fiber and the thickness of that medium.

In their study using the rat sciatic nerve, Wells et al. report a value of 0.66 J/cm^2 as the radiant exposure above which the probability of thermal damage is greater than 1%. At approximately 0.8 J/cm^2, the probability rises to 50% and at 1.2 J/cm^2 it is greater than 90%. Although their values are not directly comparable to our study given different types of tissue, the somewhat higher damage threshold they report may partly be due to the fact that they used low frequency stimulation (2 Hz) and limited the duration of INS to 8.3 minutes (1000 pulses). However, such stimulation parameters are impractical for behavioral experiments where short, high-frequency bursts of stimuli are used. In another study, Cayce et al. used 100 and 200 Hz stimulation trains at radiant exposures of up to 1.3 J/cm^2 per pulse, without any signs of functional damage, in an experimental paradigm similar to the

one in our study. (26) It is not clear in all cases whether the higher radiant exposures per pulse were used at 100 Hz or 200 Hz stimulation rates and no histological analysis was performed to rule out thermal damage at the microscopic level. A longer interstimulus interval (8 seconds, compared to the 5 seconds in our study), as well as a difference in the spot size due to variation in fiber placement could also account for some of the differences in the results. As mentioned earlier, due to the thickness of the primate cortical layer and any overlying neomembrane (which commonly develops with time following after a durotomy), the superficial damage by INS may be benign in terms of neurological function. Given the tradeoff between the increase in the functional efficacy of INS sometimes observed with higher radiant exposures, repetition rates and train durations, and the need to keep the temperature rises at a minimum, further modeling and experimental studies need to be done to determine the optimal stimulation parameters. These, of course, may vary from one experimental preparation to another. In addition to the stimulation period itself, an interstimulus interval of sufficient length must be employed to allow for any residual temperature elevation to return to baseline. The calculation of the optimal value is, again, best reserved for modeling studies.

Conclusion

We have identified the approximate thermal threshold in terms of radiant exposure measured at optical fiber tip for an infrared neural stimulation sequence of the cerebral cortex. Above this threshold, (somewhere between 0.3 and 0.4 J/cm^2), lesions are seen in histological preparations and, at radiant exposures of 0.6 J/cm^2 or higher, *in vivo* as well. However, variations in position of the fiber, geometry of fiber tip, thickness of the artificial dura, the presence of saline or agar between fiber and tissue, and amount of neomembrane growth can all reduce the effective radiant exposure at the cortical surface. These experimental differences, as well as the small size of the lesions, may account for lack of damage observed in previously published studies where suprathreshold radiant exposures were reported. (10, 21, 24)

In the range of suprathreshold radiant exposures tested (0.4–0.9 J/cm^2), the lesion had the shape of a paraboloid, with its widest part at the surface of the tissue and with the apex below the center of the fiber. As radiant exposures were increased, the apex moved deeper into the tissue, but the width of the paraboloid at the surface remained approximately the same. Histological inspection showed three distinct patterns of tissue damage within the lesion, the middle zone being most readily apparent. Given that individual stimulation pulses are usually insufficient for functional modulation of brain activity, the INS community would benefit from a theoretical model of temperature rise as a function of various stimulation sequence parameters, such as the frequency, duty cycle and duration of the stimulus. Although it is the temperature gradient rather than the actual temperature itself that is thought to be responsible for the electrophysiological effect behind INS, the DC component of the temperature rise during high frequency stimulation may be the major practical limiting factor of the technique.

Acknowledgments

The work was funded by NIH grants MH095009 and NS044275. Processing of rodent tissue was supported by the National Eye Institute Vision Core Grant: P30 EY08126. The authors would like to thank Drs. E.D. Jansen and A. Mahadevan-Jansen for the loan of the Aculight laser and for valuable discussions.

References

1. Grill WM, Norman SE, Bellamkonda RV. Implanted neural interfaces: biochallenges and engineered solutions. Annu Rev Biomed Eng. 2009; 11:1–24. [PubMed: 19400710]
2. Yizhar O, Fenno LE, Davidson TJ, Mogri M, Deisseroth K. Optogenetics in neural systems. Neuron. 2011 Jul 14; 71(1):9–34. [PubMed: 21745635]
3. Wells J, Kao C, Mariappan K, Albea J, Jansen ED, Konrad P, et al. Optical stimulation of neural tissue in vivo. Opt Lett. 2005 Mar 1; 30(5):504–6. [PubMed: 15789717]
4. Wells J, Kao C, Konrad P, Milner T, Kim J, Mahadevan-Jansen A, et al. Biophysical mechanisms of transient optical stimulation of peripheral nerve. Biophys J. 2007 Oct 1; 93(7):2567–80. [PubMed: 17526565]
5. Shapiro MG, Homma K, Villarreal S, Richter CP, Bezanilla F. Infrared light excites cells by changing their electrical capacitance. Nat Commun. 2012; 3:736. [PubMed: 22415827]
6. Yao J, Liu B, Qin F. Rapid temperature jump by infrared diode laser irradiation for patch-clamp studies. Biophys J. 2009 May 6; 96(9):3611–9. [PubMed: 19413966]
7. Albert ES, Bec JM, Desmadryl G, Chekroud K, Travo C, Gaboyard S, et al. TRPV4 channels mediate the infrared laser-evoked response in sensory neurons. J Neurophysiol. 2012 Jun; 107(12): 3227–34. [PubMed: 22442563]
8. Jenkins MW, Duke AR, Gu S, Chiel HJ, Fujioka H, Watanabe M, et al. Optical pacing of the embryonic heart. Nat Photonics. 2010 Aug 15.4:623–6. [PubMed: 21423854]
9. Duke AR, Peterson E, Mackanos MA, Atkinson J, Tyler D, Jansen ED. Hybrid electro-optical stimulation of the rat sciatic nerve induces force generation in the plantarflexor muscles. J Neural Eng. 2012 Dec.9(6):066006. [PubMed: 23186608]
10. Cayce JM, Friedman RM, Jansen ED, Mahavaden-Jansen A, Roe AW. Pulsed infrared light alters neural activity in rat somatosensory cortex in vivo. Neuroimage. 2011 Jul 1; 57(1):155–66. [PubMed: 21513806]
11. Izzo AD, Suh E, Pathria J, Walsh JT, Whitlon DS, Richter CP. Selectivity of neural stimulation in the auditory system: a comparison of optic and electric stimuli. J Biomed Opt. 2007 Mar-Apr; 12(2):021008. [PubMed: 17477715]
12. Curcio J, Petty C. The near infrared absorption spectrum of liquid water. Journal of the Optical Society of America. 1951; 41(5):1.
13. Dewey WC. Arrhenius relationships from the molecule and cell to the clinic. Int J Hyperthermia. 2009 Feb; 25(1):3–20. [PubMed: 19219695]
14. Moritz AR, Henriques FC. Studies of Thermal Injury: II. The Relative Importance of Time and Surface Temperature in the Causation of Cutaneous Burns. Am J Pathol. 1947 Sep; 23(5):695–720. [PubMed: 19970955]
15. Bec JM, Albert ES, Marc I, Desmadryl G, Travo C, Muller A, et al. Characteristics of laser stimulation by near infrared pulses of retinal and vestibular primary neurons. Lasers Surg Med. 2012 Nov; 44(9):736–45. [PubMed: 23018648]
16. Thompson AC, Wade SA, Cadusch PJ, Brown WG, Stoddart PR. Modeling of the temporal effects of heating during infrared neural stimulation. J Biomed Opt. 2013 Mar.18(3):035004. [PubMed: 23471490]
17. Thompson AC, Wade SA, Brown WG, Stoddart PR. Modeling of light absorption in tissue during infrared neural stimulation. J Biomed Opt. Jul.17(7):075002. [PubMed: 22894474]
18. Thompson A, Wade S, Pawsey N, Stoddart P. Infrared Neural Stimulation: Influence of stimulation site spacing and repetition rates on heating. IEEE Trans Biomed Eng. 2013 Jul 11.

19. Norton BJ, Bowler MA, Wells JD, Keller MD. Analytical approaches for determining heat distributions and thermal criteria for infrared neural stimulation. J Biomed Opt. 2013 Sep.18(9): 098001. [PubMed: 24002195]

20. Wells JD, Thomsen S, Whitaker P, Jansen ED, Kao CC, Konrad PE, et al. Optically mediated nerve stimulation: Identification of injury thresholds. Lasers Surg Med. 2007 Jul; 39(6):513–26. [PubMed: 17659590]

21. Chen, G.; Cayce, JM.; Ye, X.; Jansen, ED.; Mahadevan-Jansen, A.; Roe, AW., editors. SPIE Photonics West. San Francisco, CA: 2013. Optical control of the visual perception of awake non-human primate with infrared neural stimulation.

22. Jortner BS. The return of the dark neuron. A histological artifact complicating contemporary neurotoxicologic evaluation. Neurotoxicology. 2006 Jul; 27(4):628–34. [PubMed: 16650476]

23. Kepes JJ, Malone DG, Griffin W, Moral LA, Yarde WL, Jones S. Surgical “touch artefacts” of the cerebral cortex. An experimental study with light and electron microscopic analysis. Clin Neuropathol. 1995 Mar-Apr;14(2):86–92. [PubMed: 7606902]

24. Chen, G.; Cayce, JM.; Friedman, RM.; Wang, F.; Tang, C.; Jansen, ED., et al., editors. Society for Neuroscience Meeting. New Orleans, LA: 2012. Functional tract tracing in non-human primates using pulsed infrared lasers in conjunction with optical imaging and fMRI.

25. Roe, AW.; Cayce, JM.; Ye, X.; Jansen, ED.; Mahadevan-Jansen, A., editors. Society for Neuroscience Meeting. San Diego, CA: 2013. Infrared neural stimulation of visual cortex induces visual perception in awake non-human primates.

26. Cayce JM, Friedman RM, Chen G, Jansen ED, Mahadevan-Jansen A, Roe AW. Infrared neural stimulation of primary visual cortex in non-human primates. Neuroimage. 2013 (Submitted).

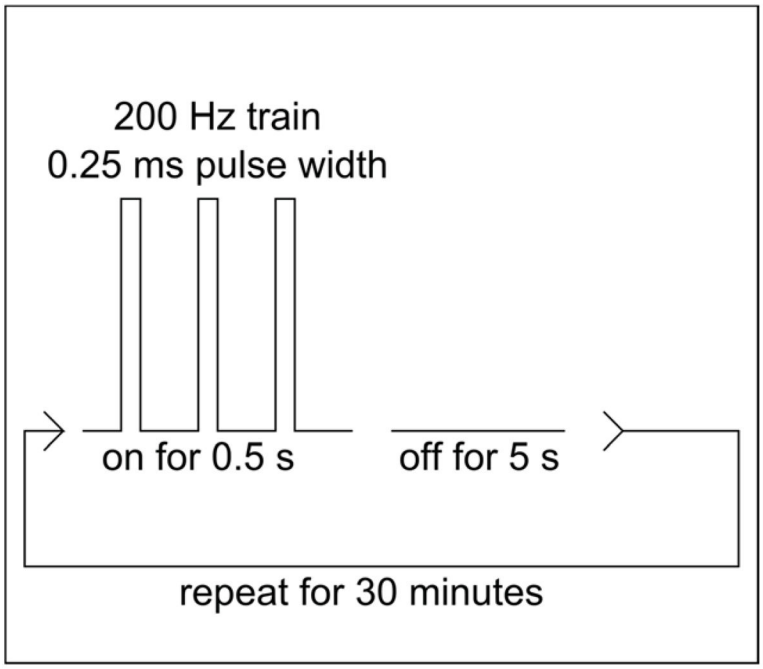

Figure 1.

INS pulse sequence. We used the INS pulse sequence shown above throughout the study, with the exception of a few trials using single high energy pulses. It consisted of high-frequency trains of laser pulses expected to modulate brain function followed by periods when the laser was off and the cortex was allowed to recover. To simplify interpretation of results, we kept the timing of the sequence constant and only varied the power (by adjusting the laser diode current) to alter the dose of radiant energy delivered to the cortex.

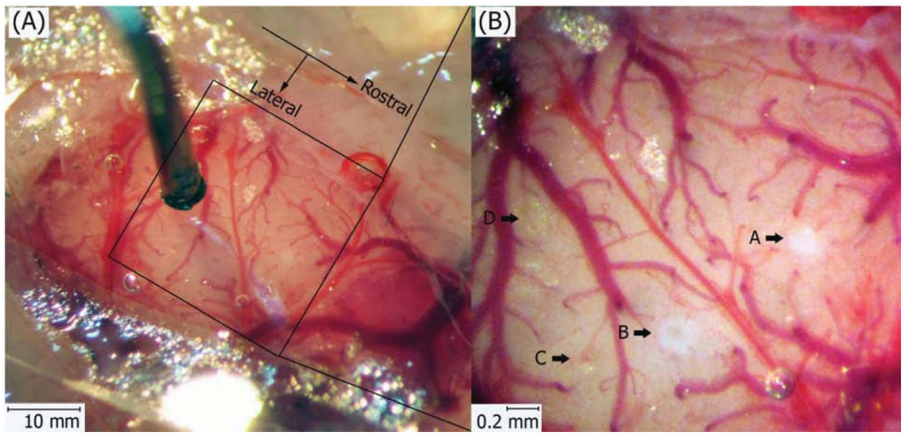

Figure 2.

INS stimulation of the rat brain *in vivo*. The figure on the right depicts the general arrangement of the stimulation setup. A craniotomy was performed over the right hemisphere and the brain is clearly visible through a transparent silicone membrane secured in place with agar. A 200 micron core optical fiber enclosed in a steel cannula to improve rigidity is positioned over the membrane,. On the right is a magnified image taken after focal INS stimulation, showing three areas subjected to INS. The radiant exposures per pulse were: A- 0.7 J/cm^2, B- 0.8 J/cm^2, C- 0.5 J/cm^2, D- 0.4 J/cm^2. Spots A and B clearly show blanching of the brain, indicating the presence of thermally induced damage.

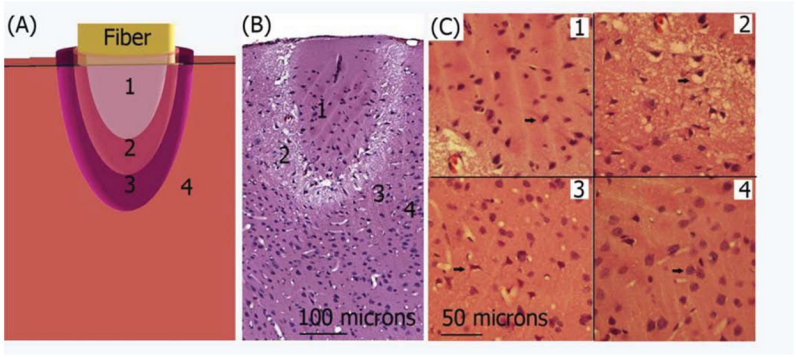

Figure 3.

Thermally induced lesion in a rat brain (A). Schematic representation of a thermally induced cortical lesion. Three visually identifiably zones of damage are labeled as 1, 2, 3. Area outside of the lesions is labeled as zone 4. B Stained sections of rat brain showing a thermally induced lesion. (B). Hematoxylin and eosin stained sections reveal a parabola-shaped lesion at the location of stimulation, with pulse energy of 0.8 J/cm^2. The three zones of damage are labeled as in (A). (C). The areas marked on (B) are shown on the right at greater magnification. The arrow in panel 4 shows the typical appearance of a neuron outside the lesion area. In 1, 2, 3, neurons have an abnormal appearance (arrows), as described in the text in greater detail.

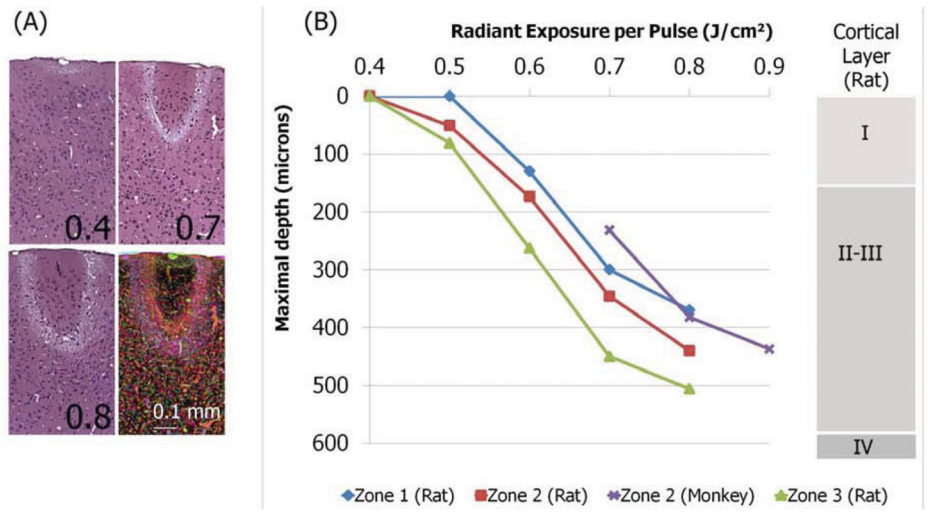

Figure 4.

The spread of thermally induced INS lesions as a function of radiant exposure. (A). Hematoxylin and eosin stained sections of thermally induced lesions following INS in the rat brain. The radiant exposures were 0.4, 0.7 and 0.8 J/cm2 per pulse, as labeled. The panel on the lower right is an overlay of the three exposures, with the photographs colored green, red and blue, respectively. (B). Quantification of the maximal spread below cortical surface of the lesions as a function of radiant exposure.

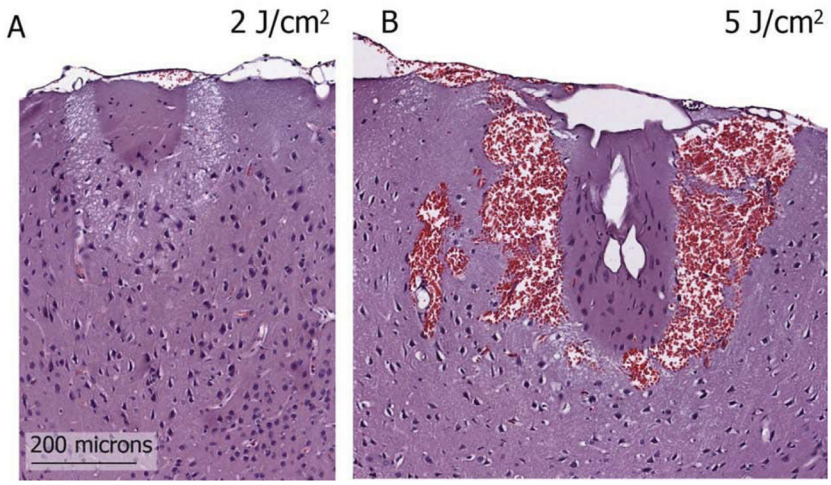

Figure 5.

Thermally induced lesions following INS in the rat brain: high energy single pulses. Shown are hematoxylin and eosin stained sections of a rat brain exposed to single INS pulses of 2 (A) and 5 (B) J/cm^2. The lower radiant exposure lesion is similar in appearance to the ones obtained using pulse sequences (see figures 2 and 3). At 5 J/cm^2, some new features emerge, such as the distortion and appearance of cavities in zone A and the filling of zone B with blood, presumably due to rupture of the vasculature.

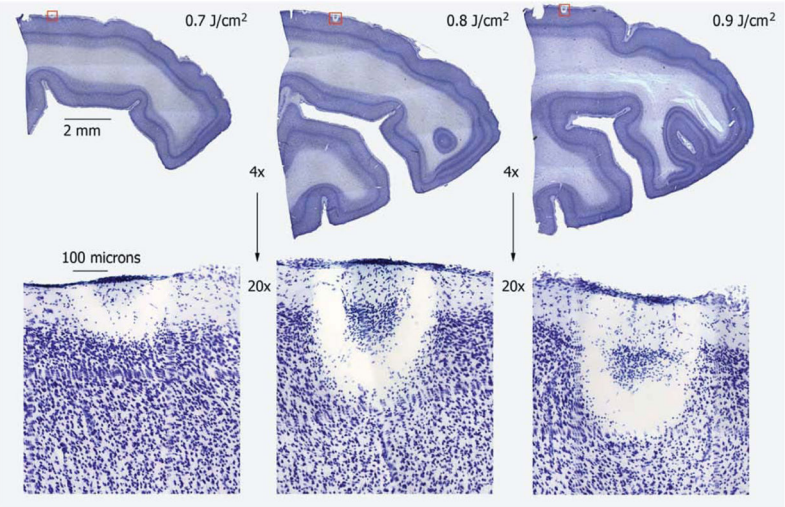

Figure 6.

Thermally induced lesions following INS of a squirrel monkey brain. Shown are representative cresyl violet- stained frozen sections of a squirrel monkey brain subjected to INS. (A–C) Histological brain slice, photographed using a 4x objective. (D–F) Magnified view of area of the lesion (red squares), taken with a 20x objective.